

# Preparation of $\beta(1 \rightarrow 3)/\beta(1 \rightarrow 4)$ -xylooligosaccharides from red alga dulse by two xylanases from *Streptomyces thermogriseus*

**Yuki Fujii**

Hokkaido University

**Manami Kobayashi**

Hokkaido University

**Yoshikatsu Miyabe**

Hokkaido University

**Hideki Kishimura**

Hokkaido University

**Tadashi Hatanaka**

Research Institute for Biological Sciences

**Yuya Kumagai** (✉ [yuyakumagai@fish.hokudai.ac.jp](mailto:yuyakumagai@fish.hokudai.ac.jp))

Hokkaido University: Hokkaido Daigaku <https://orcid.org/0000-0003-1209-9979>

---

## Research

**Keywords:** Red alga, Dulse, Xylan,  $\beta(1 \rightarrow 3)/\beta(1 \rightarrow 4)$ -Xylooligosaccharides, Endo-xylanase, *Streptomyces thermogriseus*

**Posted Date:** February 17th, 2021

**DOI:** <https://doi.org/10.21203/rs.3.rs-232757/v1>

**License:**  This work is licensed under a Creative Commons Attribution 4.0 International License.

[Read Full License](#)

---

## Abstract

Red alga dulse has xylan with the structure containing  $\beta(1\rightarrow3)/\beta(1\rightarrow4)$ -linkage. We previously prepared xylooligosaccharides (XOS) from dulse xylan, however, the product contains many D-xylose and less XOS having  $\beta(1\rightarrow3)$ -linkage. To improve the efficiency of XOS production, we prepared two recombinant endo-xylanases from *Streptomyces thermophilus* (StXyl10 and StXyl11). Comparing the  $k_{cat}/K_m$  value for dulse xylan, the value of StXyl10 was approximately two times higher than that of StXyl11. We then determined the suitable condition for XOS production. As a result, the dulse XOS was prepared by the successive hydrolysis of 10 mg/ml of dulse xylan by 0.5  $\mu$ g/ml StXyl10 for 4 h at 50°C and then 2.0  $\mu$ g/ml StXyl11 for 36 h at 60°C. The xylan was converted into 95.8% of XOS, including 59.7% of XOS having  $\beta(1\rightarrow3)$ -linkage, and 0.97% of X1. Our study provide useful information for the production of XOS having  $\beta(1\rightarrow3)$ -linkage.

## Introduction

Xylan is very useful to produce biofuel, pulp, fiber and foods (Buchert et al. 1994; Dodd et al. 2009; Duarte et al. 2012). In food industry, xylan is converted to D-xylose (X1) or xylooligosaccharides (XOS). X1 is used as a low calorie sweetness, a source for xylitol and a coloring agent by Maillard reaction (Akpinar et al. 2009). XOS are stable at low pH and high temperature up to 100°C (Carvalho et al. 2013; Singh et al. 2015). XOS shows the function as the decrease in blood sugar, lipids and oxidative status in type-2 diabetes mellitus (Gobinath et al. 2010; Sheu et al. 2008). In addition, XOS are known as prebiotics showing various beneficial effects on human health (Okazaki et al. 1990; Zhu et al. 2015).

Land plant cell walls are the complex structures consisting of cellulose, hemicellulose, pectin and lignin. Main polysaccharide of hemicelluloses is xylan and mannan. Land plant xylan forms xylan-cellulose-lignin complex by covalent and non-covalent bonds (Akpinar et al. 2009; Zhu et al. 2006; Guillaume et al. 2019), and the structure resists enzymatic hydrolysis. Therefore, pretreatments with acid or alkali are necessary for the enzymatic hydrolysis of xylan (Carvalho et al. 2013; de Figueiredo et al. 2017; Lyu et al. 2018; Rajagopalan et al. 2017). Red algae also possess cell walls with no lignin and less cellulose (Martone et al. 2009). Although main polysaccharides of red algae were usually galactan, agar and carrageenan, some red algae, Nemaliophycidae, possess xylan in their cell wall (Chen et al. 1986; Nerinckx et al. 2004). Structure of red algal xylan mainly consists of one  $\beta(1\rightarrow3)$  linkage in every  $\beta(1\rightarrow4)$  xylohexose (Deniaud et al. 2003; Nerinckx et al. 2004; Viana et al. 2011). Because of the mix-linked structure, interaction between xylosans is loose (Lahaye et al. 2003), indicating that red algal xylan has the advantages in the enzymatic production of XOS. Red alga dulse contains xylan with a minor amount of cellulose and  $\beta(1\rightarrow4)$ -xylan in the cell wall (Morgan et al. 1980). The major components of dulse is proteins (approximately 40 g/100 g dried dulse) (Furuta et al. 2016; Miyabe et al. 2017). Therefore, we have been studied the components and function on human health such as antioxidant activity and inhibitory activity of angiotensin-I-converting activity (Kumagai et al. 2019a; Kumagai et al. 2019b; Nishida et al. 2020; Sato et al. 2019). Xylan is the second main ingredient of dulse. We attempted to

prepare XOS from dulse xylan using commercial enzymes (Yamamoto et al. 2019). Then, we purified  $\beta(1\rightarrow3)$  xylosyl xyllobiose (DX3) and clarified prebiotics on *Bifidobacterium* sp. (Kobayashi et al. 2020).

Endo-1,4- $\beta$ -xylanase (EC 3.2.1.8) is one of the main enzymes for xylan hydrolysis (Chapla et al. 2012). The enzyme is mainly classified into glycoside hydrolase families (GH, <http://www.cazy.org/>) 10 and GH11 (Álvarez-Cervantes et al. 2016; Paës et al. 2012; Yagi et al. 2019). GH10 folds  $(\beta/\alpha)_8$  barrel structure and hydrolyzes xylan having side chain (Biely et al. 1997). The hydrolysis products by GH10 were X1 and the XOS having the short degree of polymerization (DP) (Meng et al. 2015; Rahmani et al. 2019). GH11 folds  $\beta$ -jelly roll structure, and the enzyme also hydrolyzed xylan having side chains. The hydrolysis products were XOS having large DP and less X1. The difference of hydrolysis products came from the enzyme structures. GH10 xylanases usually possess 5 to 7 subsites. These subsites incorporate X1 having side chains of  $\alpha(1\rightarrow3)$ -arabinofuranose and  $\alpha(1\rightarrow2)$ -4-O-methylglucuronic acid except for subsite -1 (Fujimoto et al. 2004). Subsites of GH11 xylanases usually possess subsites -2 to +3, and subsites -2 to +1 did not incorporate X1 having side chains (Vardakou et al. 2008). The use of xylanases having different substrate specificities would lead to the efficient production of XOS having  $\beta(1\rightarrow3)$  linkage.

In this study, we prepared and characterized GH10 and GH11 endo-xylanases from *S. thermogriseus* (StXyl10 and StXyl11). Next, we attempted to produce XOS having less X1 and much  $\beta(1\rightarrow3)$  linkage from dulse xylan by using the two characteristic xylanases.

## Results And Discussion

### Cloning and sequence analysis of xylanases from *S. thermogriseus*

Sequencing of the genomic DNA of *S. thermogriseus* NBRC100772 was performed using a PacBio next generation sequencer, and their annotations were performed by the Prokka program. Using PCR methods, two *S. thermogriseus* xylanase genes (stxyl10 and stxyl11) were cloned. Consequently, we determined nucleotide sequences of 1,434 bp for stxyl10 encoding the amino-acid sequence of 477 residues and 996 bp for stxyl11 encoding the amino-acid (AA) sequence of 331 residues. The signal peptide for the secretion was predicted by the SignalP 4.1 server (<http://www.cbs.dtu.dk/services/SignalP-4.1/>). StXyl10 consists of 1–41 AA residues for signal peptide and 42–477 AA residues for mature protein composed of GH10 catalytic domain, linker and CBM13. StXyl11 consists of 1–41 AA residues for signal peptide and 42–331 AA residues for mature protein composed of GH11 catalytic domain, linker and CBM2. StXyl10 showed the 99.8% identity with GH10 *Streptomyces thermophilus* TISTR1948 xylanase (NCBI accession number (AN): LC088500) and XynST10 from *Streptomyces* sp. B6 (AN: MN420656) (Boonchuay et al. 2016; Chaiyaso et al. 2011; Liu et al. 2020). The CBM2 of StXyl10 was substituted Ile475 with Thr475 to compare above enzymes. The primary structure of StXyl11 showed the 100% identity with GH11 from *Streptomyces* sp. B6 XynST11 (AN: MN420657) and 99.3% identity with one from *Streptomyces thermophilus* NTU-88 (AN: ABF72145), which is named as *S. thermophilus* in NCBI (Cheng et al. 2008).

## Biochemical characterization of xylanases

StXyl10 and StXyl11 were expressed in *Escherichia coli*. The purities of xylanases were evaluated by SDS-PAGE (Fig. 1). StXyl10 showed two bands with the molecular weights of 38,600 and 46,900. The deduced molecular weight of StXyl10 with 6×His-tag was 46,990, which was corresponded to the large band. We therefore thought that the large band was mature StXyl10. The expressed enzymes in this study possessed 6×His-tag at the N-terminus. The small band was estimated the loss of approximately 30 AA from C-terminus. CBM13 is consisted of approximately 150 AA. It was reported that the N-terminus of CBM13 was required for the substrate binding (PDB: 1V6X) (Fujimoto et al. 2004). In addition, the small band did not find in the purified StXyl11, meaning that this was not come from bacterial contamination. Catalytic domain of StXyl10 was remained in the small band. We regards the two bands as StXyl10. StXyl11 showed a single band at 32,400 MW, which was the same as the deduced molecular weight of 32,409 containing 6 × His-tag.

The optimal temperatures of StXyl10 and StXyl11 were 70 °C and 60 °C, respectively (Fig. 2a). The optimal pH of StXyl10 and StXyl11 were pH 5.0–8.0 and pH 6.0–7.0, respectively (Fig. 2b). StXyl10 was stable at 50 °C for 24 h. The thermal stability of StXyl10 at 60 °C was decreased in 27% for 12 h. The half inactivation of StXyl10 at 70 °C was 3.3 min. Thermal stabilities of StXyl11 at 50 °C and 60 °C for 24 h were 70% and 52%, respectively (Fig. 2c). In the optimal condition, StXyl10 and StXyl11 showed the specific activity of 252 U/mg at 70 °C and 1,392 U/mg at 60 °C, respectively. These enzymatic characters were similar to mesophilic Streptomyces xylanases (Boonchuay et al. 2016; Chaiyaso et al. 2011; Cheng et al. 2008; Liu et al. 2020).

Kinetic parameters of StXyl10 for GX and DX were 675 and 858 sec/(mg/ml), respectively (Table 1). Those of StXyl11 for GX and DX were 610 and 445 ml/mg/sec, respectively. Comparing DX parameter of StXyl10 and StXyl11, the  $k_{cat}/K_m$  value of StXyl10 was approximately two times high. This is the first report that measuring kinetic parameter toward DX.

## Substrate specificities of xylanases

Hydrolysis products of AX, GX and DX by StXyl10 and StXyl11 were evaluated by TLC (Fig. 3). Hydrolysis products by StXyl10 were composed of X1 and XOS having short DP, DP2-DP4. Imaging analysis showed that the ratio of main hydrolysis products of DX were as follows: X2, 23.2%; DX3, 25.2% and DX4, 27.6%. On the other hand, main hydrolysis products by StXyl11 showed the XOS larger than DP4. The hydrolysis products of StXyl11 did not contained X1 from the three substrates and DX3 from DX. From the results, StXyl10 produced shorter DP than StXyl11 among the three substrates.

## Hydrolysis products by using xylanases

For the efficient production of XOS from DX without producing X1, the hydrolysates by StXyl10 and StXyl11 were evaluated (Table 3). We first determined the reaction condition of enzyme concentration and reaction time for each enzyme. To evaluate enzyme concentrations, DX was hydrolyzed for 4 h at the

concentration of 0.1–2.0 µg/ml StXyl10 and for 24 h at the concentration of 0.5–8.0 µg/ml StXyl11. To evaluate the reaction times, DX was hydrolyzed at 0.5 µg/ml StXyl10 for 1–12 h and 2.0 µg/ml StXyl11 for 1–36 h. The hydrolysis products were separated by TLC, and the amounts of X1 and DX were evaluated by the density.

When DX was hydrolyzed for 4 h at the concentration of 0.1–2.0 µg/ml StXyl10, the relationship between a decrease of DX and an increase of X1 was found except for the concentration of 0.1 µg/ml StXyl10, which would remain large DP substrates at the origin of TLC (Table 3). X1 spot was clearly found in the hydrolysate by 1.0 µg/ml StXyl10. Therefore, we selected the concentration of 0.5 µg/ml StXyl10 to evaluate the reaction time. Then, reaction time was evaluated from 1 to 24 h. Although the amount of X1 up to 4 h was stable, the amount of X1 was increased without a decrease of DX in the hydrolysate from 4 to 12 h reaction. From these results, we determined the DX hydrolysis condition as 0.5 µg/ml StXyl10 for 4 h.

Then, DX hydrolysis conditions by StXyl11 were evaluated. When DX was hydrolyzed for 24 h at the concentration of 0.5–8.0 µg/ml StXyl11, a decrease of DX was faster than an increase of X1 up to 2.0 µg/ml StXyl11 (Table 3). A decrease of DX was slower than an increase of X1 from 2.0 to 8.0 µg/ml StXyl11. Therefore, we selected the concentration of 2.0 µg/ml StXyl11 to evaluate the reaction time. Then, reaction time was evaluated from 1 to 36 h. Although the amount of X1 was low in the tested times, the amount of DX was decreased up to 24 h and almost unchanged for 36 h.

The hydrolysates by the above conditions were confirmed by gel filtration. The hydrolysate by StXyl10 did not contain X1 but the product remained larger DP (fractions 16-22). On the other hand, the hydrolysate by StXyl11 contained XOS, but it still remained unhydrolyzed DX (Fig. 4a). The amount of intact DX was 8.2% in the hydrolysate by StXyl10 and 12.4% in the hydrolysate by StXyl11. We therefore evaluated the successive hydrolysis of DX by StXyl10 and StXyl11.

### **Successive hydrolysis of DX by two xylanases**

For the successive hydrolysis of DX, the hydrolysis condition of StXyl10, which was determined in the previous section (0.5 µg/ml StXyl10 for 4 h), was employed for the limited degradation. After the denature of StXyl10 at 100 °C for 10 min, the second hydrolysis condition was evaluated using the information from previous section (0.5 or 2.0 µg/ml StXyl11 for 24 or 36 h) (Table 4). Although the amount of X1 did not increase in the tested conditions, the amount of DX was decreased in the sample of 36 h hydrolysis (Table 4). The sample, prepared by 2.0 µg/ml StXyl11 for 36 h, contained less DX in the tested conditions. Therefore, we determined the successive hydrolysis conditions as follows: 0.5 µg/ml StXyl10 for 4 h and then 2.0 µg/ml StXyl11 for 36 h. The composition of hydrolysis products was evaluated in the next section.

### **Evaluation of hydrolysis product by the combination of two xylanases**

The hydrolysis ratio of the sample was determined by measuring the amount of remaining intact DX by gel filtration. The intact DX was detected in the fractions 11-15 (Fig. 4b). We confirmed that the amount of sugars in fractions 11-35 was corresponded to that of the applied sugars. Therefore, we determined that the intact DX in the hydrolysate was remained 3.3% in fractions 11-15. This means that 96.7% of DX was hydrolyzed.

The hydrolysis products of the sample were subjected to HPLC. Since X1 peak in HPLC was overlap with injection peaks, we used D-xylose analysis kit for the quantity of X1. The amount of X1 in the sample was 0.94%, meaning that X1 was hardly detectable. The sample contained X2-X4, DX3 and DX4. The peaks eluted later than X4 would be XOS containing  $\beta(1\rightarrow 3)$  linkage because of DX structure and substrate specificities of xylanases (Biely et al. 1997). We previously reported the structures of DX3 and DX4 (Yamamoto et al. 2019). The structures of DX4 showed two patterns, i.e., Xyl- $\beta(1\rightarrow 3)$ -Xyl- $\beta(1\rightarrow 4)$ -Xyl- $\beta(1\rightarrow 4)$ -Xyl and Xyl- $\beta(1\rightarrow 4)$ -Xyl- $\beta(1\rightarrow 3)$ -Xyl- $\beta(1\rightarrow 4)$ -Xyl. Therefore, we classified the larger XOS into two patterns, DX6-1, DX7-1: XOS having  $\beta(1\rightarrow 3)$  linkage in the middle and DX6-2, DX7-2: XOS having  $\beta(1\rightarrow 3)$  linkage at the non-reducing terminus, and estimated the DP from their retention time (Fig. 5). From these results, the composition of XOS contained mainly DX4 (21.3%), DX5 (18.6%), X3 (18.4%) and X2 (15.5%). The product contained less X1 (0.94%). The hydrolysis ratio of DX was 96.7%, and the yield of XOS was 95.8%. The ratio of XOS having  $\beta(1\rightarrow 3)$  linkage was 59.7%, resulting in the effective production of unique XOS.

We previously prepared XOS from DX using commercial enzyme hemicellulase amano 90. The product contained 15.0% X1 with the hydrolysis ratio of 82.0% (Yamamoto et al. 2019). The main products of hemicellulase amano 90 were X1 and X2 and contained less XOS having  $\beta(1\rightarrow 3)$  linkage (40%). The preparation method in this study was suitable for producing XOS having  $\beta(1\rightarrow 3)$  linkage, which was increased from 40% to 59.7%.

## Conclusions

Red alga dulse contains  $\beta(1\rightarrow 3)/\beta(1\rightarrow 4)$  linkage in the xylan. Oligosaccharides having different structure showed the different biological function. Our previous preparation method contained many X1 and less  $\beta(1\rightarrow 3)$  linked XOS. This study showed the efficient XOS production by the successive hydrolysis using two endo-xylanases (0.5  $\mu$ g/ml StXyl10 for 4 h at 50°C and then 2.0  $\mu$ g/ml StXyl11 for 36 h at 60°C). The composition of the product was as follows, 0.97% of X1 and 95.8% of XOS containing 59.7% of  $\beta(1\rightarrow 3)$  linked XOS. Our study provide useful information for the production of  $\beta(1\rightarrow 3)$  linked XOS.

## Materials And Methods

### Materials

Dulse (*Palmaria palmata* in Japan) was harvested at Usujiri, Hokkaido, Japan and stored at -30 °C until use (Yamamoto et al. 2019; Kobayashi et al. 2020). Xylose (X1), xylobiose (X2) and xylotriose (X3) were

purchased from Wako Pure Chemical Industries (Osaka, Japan). Xylotetraose (X4), xylopentaose (X5), beechwood xylan (GX) and arabinoxylan (wheat flour; insoluble) (AX) were purchased from Megazyme (Bray, Ireland). Sugar-D column (4.6 × 250 mm) was purchased from Nakalai Tesque (Kyoto, Japan). Superdex Peptide 10/300 GL column was from GE Healthcare (Tokyo, Japan). Genome DNA of *S. thermogriseus* NBRC 100772 was obtained from the NITE Biological Resource Center (NBRC). Other reagents were obtained from Wako Pure Chemical Industries Ltd. (Osaka, Japan).

### **Preparation of dulse xylan**

Dulse xylan (DX) was prepared as previously (Yamamoto et al. 2019). Namely, frozen dulse was lyophilized and homogenized into powder. The powder was delipidated with chloroform-methanol (1:2, v/v) and then dried. Dulse xylan was extracted from the delipidated powder. The powder was suspended in 40-volumes (v/w) of distilled water and autoclaved at 121 °C for 20 min. The sample of supernatant was mixed with urea (8 M final concentration), centrifugated and then dialyzed against distilled water using a dialysis tube (molecular weight cut off: approximately 14 kDa, EIDIA Co., Ltd., Tokyo, Japan). The solution was centrifuged at 15,000×g for 5 min to remove small amounts of insoluble materials, and the supernatant was lyophilized. Then, the sample was dissolved in water (10 mg/ml) and purified with 80% ethanol precipitation. The dried precipitate was used as dulse xylan (DX). The DP of dulse xylan was determined by the amount of total sugar and reducing sugar by the methods of phenol sulfate method (Dubois et al. 1951) and 3,5-dinitrosalicylic acid method (DNS) (Miller 1959), respectively. The purity of the prepared DX contained 30.8% X1 and the average DP was 29.

### **Preparation of xylanases**

The genes encoding xylanase, StXyl10 (DNA Data Bank of Japan AN: LC603131) and StXyl11 (AN: LC603130), were amplified by polymerase chain reaction (PCR) using genomic DNA of *S. thermogriseus* as a template and the sets of primers: 5'- ACATATGGCCGAGAGCACACTCGGCGC-3' (StXyl10-forward) and 5'- TAAGCTTCAGGTGCGGATCCAGCGCT-3' (StXyl10-reverse), 5'- ACATATGGACACCTACGTCGACACGAACCA-3' (StXyl11-forward) and 5'- TAAGCTTCAGCTCGTACTGCAGGAGACCG-3' (StXyl11-reverse), where underlines indicate the restriction enzyme sites. Then, the genes were cloned into the *NdeI-HindIII* site of pET28a to construct expression vectors of pET28a(StXyl10) and pET28a(StXyl11). The recombinant proteins were expressed in *Escherichia coli* BL21 (DE3) cells (Agilent Technologies, Palo Alto, CA, USA) harboring each expression vector, and purified as previously described (Kumagai et al. 2011). The purity of the proteins was confirmed by SDS-PAGE. The protein concentrations were determined by absorbance at 280 nm using each molar extinction coefficient.

### **Xylanase activity**

Xylanase activity was determined by the method of DNS measuring the amount of releasing reducing sugars by the reaction of 10 mg/ml BX, 1.0 µg/ml StXyl10 or StXyl11, 10 mM sodium phosphate buffer (pH 6.5) at 60 °C for 10 min. One unit of xylanase was defined as the amount of enzyme that liberates

reducing sugars equivalent to 1.0  $\mu$ mol X1 per minute. The optimal pH of xylanases was determined using 10 mM sodium citrate buffer for pH 4.0–6.0, 10 mM sodium phosphate for pH 6.0, 10 mM Tris–HCl buffer for pH 8.0 and 10 mM glycine-NaOH buffer for pH 9.0–10.0 at 60 °C for 10 min. The optimal temperature was determined at 30–80 °C using 10 mM sodium phosphate buffer (pH 6.5) for 10 min. Thermal stability of xylanases was assessed by heat treatment at 50–70 °C for 0–24 h in 10 mM sodium phosphate buffer (pH 6.5). The remaining activity was measured at the standard condition. The kinetic parameters of xylanases for xylan were determined by Michaelis–Menten equation using Origin 6.0 software (OriginLab Corporation, USA). The activity was assayed in 10 mM sodium phosphate buffer (pH 6.5) at 60 °C containing 0.25–20.0 mg/mL GX or DX. All the activity assays were performed in triplicate.

### Hydrolysis of xylan

Hydrolysis of xylan (AX, DX and GX) was performed in the reaction mixture containing 10 mM sodium phosphate (pH 6.5) and 10 mg/ml xylan for 24 h at 50 °C for 1.0  $\mu$ g/ml StXyl10 and at 60 °C for 1.0  $\mu$ g/ml StXyl11. To determine the hydrolysis condition of DX, 10 mg/ml DX was hydrolyzed in 10 mM sodium phosphate (pH 6.5) at 50 °C by 0.1–2.0  $\mu$ g/ml StXyl10 for 4 h and 0.5  $\mu$ g/ml StXyl10 for 1–12 h. Evaluation of hydrolysis of DX condition by StXyl11 was performed in 10 mg/ml DX, 10 mM sodium phosphate (pH 6.5) at 60 °C by 0.5–8.0  $\mu$ g/ml StXyl11 for 24 h and 2.0  $\mu$ g/ml StXyl11 for 1–36 h. Evaluation of the successive hydrolysis of DX by StXyl10 and StXyl11 was performed in two steps. First, 10 mg/ml DX was hydrolyzed in 10 mM sodium phosphate (pH 6.5) at 50 °C by 0.5  $\mu$ g/ml StXyl10 for 4 h. Then, StXyl10 was inactivated by heating at 100 °C for 5 min. The hydrolysate was hydrolyzed at 60 °C by 0.5 or 2.0  $\mu$ g/ml StXyl11 for 24 or 36 h.

### Thin-layer chromatography

Hydrolysis products of xylan were analyzed by TLC using a silica gel 60 plate (Merck KGaA, Darmstadt, Germany). The products were developed two times with a 2:1:1 (v/v/v) mixture of 1-butanol, acetic acid, and water. The products were detected by spraying 2:2:100:15 (w/v/v/v) mixture of diphenylamine, aniline, acetone and 80% phosphate, followed by heating at 100 °C for 10 min using the dry heat block. X1-X3, DX3 and DX4 were used as standards. The amounts of products were semi-quantitatively evaluated by imaging using Image J (Wayne Rasband (NIH), USA). The image of the detected TLC plate was converted to grayscale and invert. Then, the amounts of products were evaluated from the density.

### Evaluation of hydrolysis products

The distribution of hydrolysis products was analyzed using high performance liquid chromatography (HPLC) with a Superdex Peptide 10/300 GL column pre-equilibration with 0.3 M NaCl as previously (Kumagai et al. 2016). The samples were eluted at 0.5 ml/min and fractionated by every 1 min. The amount of sugars was determined by phenol-sulfate method. Hydrolysis ratio of DX was determined as follows: (the amount of unhydrolyzed DX / the amount of intact DX) × 100 (%).

The distribution of oligosaccharides was analyzed using HPLC equipped with a Sugar-D column (4.6 × 250 mm, Nakalai Tesque, Kyoto, Japan) with the column oven temperature at 40 °C. The products were eluted with an isocratic elution system of acetonitrile/water (4:1, v/v) at a flow rate of 1.0 ml/min and detected RI detector. X1-X3, DX3 and DX4 were used as standards. The amount of X1 was determined using D-xylose analysis kit (Megazyme, Ireland).

## Abbreviations

AN: Accession Number; DP: Degree of polymerization; DX: Dulse xylan; DX3:  $\beta(1\rightarrow3)$  Xylosyl xylobiose; DX4-DX6: XOS containing  $\beta(1\rightarrow3)$  xylosyl linkage; HPLC: High-performance liquid chromatography; StXyl10: GH10 xylanase from *S. thermogriseus*; StXyl11: GH11 xylanase from *S. thermogriseus*; TLC: Thin-layer chromatography; X2-X4:  $\beta(1\rightarrow4)$  XOS; XOS: xylooligosaccharides;

## Declarations

### Acknowledgements

We gratefully acknowledge the sampling assistant of *Palmaria palmata* in Japan at Usujiri by Professor Hiroyuki Munehara and Mr. Atsuya Miyajima.

### Authors' contributions

YF, MK, YM, MK, HK, TH and YK conceived the project. YK and TH prepared bacterial expression constructs. MK prepared dulse XOS. YF carried out all experiments. YM, YK, TH and HK wrote the manuscript. All authors read and approved the final manuscript.

### Funding

This study was supported in part by MEXT/JSPS KAKENHI (grant number 18K05810).

### Availability of data and materials

All data generated or analyzed during this study are included in this published article.

### Ethics approval and consent to participate

Not applicable.

### Consent for publication

Not applicable.

### Competing interests

The authors declare that they have no competing interests.

## Author details

<sup>1</sup>Chair of Marine Chemical Resource Development, Graduate School of Fisheries Sciences, Hokkaido University, Hakodate, Hokkaido 041-8611, Japan. <sup>2</sup>Food Research Institute, Aomori Prefectural Industrial Technology Research Center, 221-10 Yamaguchi, Nogi, Aomori-shi, Aomori-ken, 030-0142, Japan.  
<sup>3</sup>Laboratory of Marine Chemical Resource Development, Faculty of Fisheries Sciences, Hokkaido University, Hakodate, Hokkaido 041-8611, Japan. <sup>4</sup>Okayama Prefectural Technology Center for Agriculture, Forestry, and Fisheries, Research Institute for Biological Sciences (RIBS), 7549-1 Kibichuo-cho, Kaga-gun, Okayama 716-1241, Japan.

## References

- Akpınar O, Erdogan K, Bostancı S (2009) Production of xylooligosaccharides by controlled acid hydrolysis of lignocellulosic materials. *Carbohydr Res* 344:660–666.  
<https://doi.org/https://doi.org/10.1016/j.carres.2009.01.015>
- Álvarez-Cervantes J, Díaz-Godínez G, Mercado-Flores Y, et al (2016) Phylogenetic analysis of  $\beta$ -xylanase SRXL1 of *Sporisorium reilianum* and its relationship with families (GH10 and GH11) of Ascomycetes and Basidiomycetes. *Sci Rep* 6:24010. <https://doi.org/10.1038/srep24010>
- Biely P, Vršanská M, Tenkanen M, Kluepfel D (1997) Endo- $\beta$ -1,4-xylanase families: differences in catalytic properties. *J Biotechnol* 57:151–166. [https://doi.org/https://doi.org/10.1016/S0168-1656\(97\)00096-5](https://doi.org/https://doi.org/10.1016/S0168-1656(97)00096-5)
- Boonchuay P, Takenaka S, Kuntiya A, et al (2016) Purification, characterization, and molecular cloning of the xylanase from *Streptomyces thermophilus* TISTR1948 and its application to xylooligosaccharide production. *J Mol Catal B Enzym* 129:61–68.  
<https://doi.org/https://doi.org/10.1016/j.molcatb.2016.03.014>
- Buchert J, Tenkanen M, Kantelin A, Viikari L (1994) Application of xylanases in the pulp and paper industry. *Bioresour Technol* 50:65–72. [https://doi.org/https://doi.org/10.1016/0960-8524\(94\)90222-4](https://doi.org/https://doi.org/10.1016/0960-8524(94)90222-4)
- Carvalho AFA, de Oliva Neto P, da Silva DF, Pastore GM (2013) Xylo-oligosaccharides from lignocellulosic materials: Chemical structure, health benefits and production by chemical and enzymatic hydrolysis. *Food Res Int* 51:75–85. <https://doi.org/https://doi.org/10.1016/j.foodres.2012.11.021>
- Chaiyaso T, Kuniya A, Techapun C, et al (2011) Optimization of Cellulase-Free Xylanase Production by Thermophilic *Streptomyces thermophilus* TISTR1948 through Plackett-Burman and Response Surface Methodological Approaches. *Biosci Biotechnol Biochem* 75:531–537.  
<https://doi.org/10.1271/bbb.100756>
- Chapla D, Pandit P, Shah A (2012) Production of xylooligosaccharides from corncob xylan by fungal xylanase and their utilization by probiotics. *Bioresour Technol* 115:215–221.  
<https://doi.org/https://doi.org/10.1016/j.biortech.2011.10.083>

Chen WP, Matsuo M, Yasui T (1986)  $\beta$ -1,3-Xylanase and  $\beta$ -1,4-Xylanase Action on Rhodymenan. Agric Biol Chem 50:1195–1200. <https://doi.org/10.1271/bbb1961.50.1195>

Cheng H-L, Wang P-M, Chen Y-C, et al (2008) Cloning, characterization and phylogenetic relationships of stxI, a endoxylanase-encoding gene from *Streptomyces thermonitrificans* NTU-88. Bioresour Technol 99:227–231. <https://doi.org/https://doi.org/10.1016/j.biortech.2006.11.023>

de Figueiredo FC, Carvalho AFA, Brienz M, et al (2017) Chemical input reduction in the arabinoxylan and lignocellulose alkaline extraction and xylooligosaccharides production. Bioresour Technol 228:164–170. <https://doi.org/https://doi.org/10.1016/j.biortech.2016.12.097>

Deniaud E, Quemener B, Fleurence J, Lahaye M (2003) Structural studies of the mix-linked  $\beta$ -(1→3)/ $\beta$ -(1→4)-d-xylans from the cell wall of *Palmaria palmata* (Rhodophyta). Int J Biol Macromol 33:9–18. [https://doi.org/https://doi.org/10.1016/S0141-8130\(03\)00058-8](https://doi.org/https://doi.org/10.1016/S0141-8130(03)00058-8)

Dodd D, Cann IKO (2009) Enzymatic deconstruction of xylan for biofuel production. GCB Bioenergy 1:2–17. <https://doi.org/https://doi.org/10.1111/j.1757-1707.2009.01004.x>

Duarte G, Moreira L, Gómez-Mendoza D, et al. (2012) Use of Residual Biomass from the Textile Industry as Carbon Source for Production of a Low-Molecular-Weight Xylanase from *Aspergillus oryzae*. Applied Sciences 2:754–772. doi: 10.3390/app2040754

Dubois M, Gilles K, Hamilton JK, et al (1951) A Colorimetric Method for the Determination of Sugars. Nature 168:167. <https://doi.org/10.1038/168167a0>

Fujimoto Z, Kaneko S, Kuno A, et al (2004) Crystal Structures of Decorated Xylooligosaccharides Bound to a Family 10 Xylanase from *Streptomyces olivaceoviridis* E-86. J Biol Chem 279:9606–9614. <https://doi.org/10.1074/jbc.M312293200>

Furuta T, Miyabe Y, Yasui H, et al. (2016) Angiotensin I Converting Enzyme Inhibitory Peptides Derived from Phycobiliproteins of Dulse *Palmaria palmata*. Mar Drugs 14:32. doi: 10.3390/md14020032

Gobinath D, Madhu AN, Prashant G, et al (2010) Beneficial effect of xylo-oligosaccharides and fructo-oligosaccharides in streptozotocin-induced diabetic rats. Br J Nutr 104:40–47. <https://doi.org/10.1017/S0007114510000243>

Guillaume A, Thorigné A, Carré Y, et al (2019) Contribution of proteases and cellulases produced by solid-state fermentation to the improvement of corn ethanol production. Bioresour Bioprocess 6:7. <https://doi.org/10.1186/s40643-019-0241-0>

Kobayashi M, Kumagai Y, Yamamoto Y, et al. (2020) Identification of a Key Enzyme for the Hydrolysis of  $\beta$ -(1→3)-Xylosyl Linkage in Red Alga Dulse Xylooligosaccharide from *Bifidobacterium adolescentis*. Mar Drugs 18:174. doi: 10.3390/md18030174

Kumagai Y, Usuki H, Yamamoto Y, et al (2011) Characterization of calcium ion sensitive region for  $\beta$ -Mannanase from *Streptomyces thermophilic*. Biochim Biophys Acta - Proteins Proteomics 1814:1127–1133. <https://doi.org/https://doi.org/10.1016/j.bbapap.2011.04.017>

Kumagai Y, Okuyama M, Kimura A (2016) Heat treatment of curdlan enhances the enzymatic production of biologically active  $\beta$ -(1,3)-glucan oligosaccharides. Carbohydr Polym 146:396–401. <https://doi.org/https://doi.org/10.1016/j.carbpol.2016.03.066>

Kumagai Y, Miyabe Y, Takeda T, et al. (2019a) *In Silico* Analysis of Relationship between Proteins from Plastid Genome of Red Alga *Palmaria* sp. (Japan) and Angiotensin I Converting Enzyme Inhibitory Peptides. Mar Drugs 17:190. doi: 10.3390/md17030190

Kumagai Y, Tsubouchi R, Miyabe Y, et al (2019b) Complete sequence of mitochondrial DNA of red alga dulse *Palmaria palmata* (Linnaeus) Weber & Mohr in Japan. Mitochondrial DNA Part B 4:3177–3178. <https://doi.org/10.1080/23802359.2019.1668733>

Lahaye M, Rondeau-Mouro C, Deniaud E, Buléon A (2003) Solid-state  $^{13}\text{C}$  NMR spectroscopy studies of xylans in the cell wall of *Palmaria palmata* (L. Kuntze, Rhodophyta). Carbohydr Res 338:1559–1569. [https://doi.org/https://doi.org/10.1016/S0008-6215\(03\)00241-6](https://doi.org/https://doi.org/10.1016/S0008-6215(03)00241-6)

Liu L, Xu M, Cao Y, et al (2020) Biochemical Characterization of Xylanases from *Streptomyces* sp. B6 and Their Application in the Xylooligosaccharide Production from Viscose Fiber Production Waste. J Agric Food Chem 68:3184–3194. <https://doi.org/10.1021/acs.jafc.9b06704>

Lyu H, Zhou J, Geng Z, et al (2018) Two-stage processing of liquid hot water pretreatment for recovering C5 and C6 sugars from cassava straw. Process Biochem 75:202–211. <https://doi.org/https://doi.org/10.1016/j.procbio.2018.10.003>

Martone PT, Estevez JM, Lu F, et al (2009) Discovery of Lignin in Seaweed Reveals Convergent Evolution of Cell-Wall Architecture. Curr Biol 19:169–175. <https://doi.org/https://doi.org/10.1016/j.cub.2008.12.031>

Meng D-D, Ying Y, Chen X-H, et al (2015) Distinct Roles for Carbohydrate-Binding Modules of Glycoside Hydrolase 10 (GH10) and GH11 Xylanases from *Caldicellulosiruptor* sp. Strain F32 in Thermostability and Catalytic Efficiency. Appl Environ Microbiol 81:2006–2014. <https://doi.org/10.1128/AEM.03677-14>

Miller GL (1959) Use of Dinitrosalicylic Acid Reagent for Determination of Reducing Sugar. Anal Chem 31:426–428. <https://doi.org/10.1021/ac60147a030>

Miyabe Y, Furuta T, Takeda T, et al (2017) Structural Properties of Phycoerythrin from Dulse *Palmaria palmata*. J Food Biochem 41:.. <https://doi.org/10.1111/jfbc.12301>

Morgan KC, Wright JLC, Simpson FJ (1980) Review of chemical constituents of the red alga *Palmaria palmata* (dulse). Econ Bot 34:27–50. <https://doi.org/10.1007/BF02859553>

Nerinckx W, Broberg A, Duus JØ, et al (2004) Hydrolysis of *Nothogenia erinacea* xylan by xylanases from families 10 and 11. Carbohydr Res 339:1047–1060.

<https://doi.org/https://doi.org/10.1016/j.carres.2004.02.017>

Nishida Y, Kumagai Y, Michiba S, et al. (2020) Efficient Extraction and Antioxidant Capacity of Mycosporine-Like Amino Acids from Red Alga Dulse *Palmaria palmata* in Japan. Marine Drugs 18:502. doi: 10.3390/md18100502

Okazaki M, Fujikawa S, Matsumoto N (1990) Effect of Xylooligosaccharide on the Growth of Bifidobacteria. Bifidobact Microflora 9:77–86. [https://doi.org/10.12938/bifidus1982.9.2\\_77](https://doi.org/10.12938/bifidus1982.9.2_77)

Paës G, Berrin J-G, Beaugrand J (2012) GH11 xylanases: Structure/function/properties relationships and applications. Biotechnol Adv 30:564–592.

<https://doi.org/https://doi.org/10.1016/j.biotechadv.2011.10.003>

Rahmani N, Kahar P, Lisdiyanti P, et al (2019) GH-10 and GH-11 Endo-1,4- $\beta$ -xylanase enzymes from *Kitasatospora* sp. produce xylose and xylooligosaccharides from sugarcane bagasse with no xylose inhibition. Bioresour Technol 272:315–325.

<https://doi.org/https://doi.org/10.1016/j.biortech.2018.10.007>

Rajagopalan G, Shanmugavelu K, Yang K-L (2017) Production of prebiotic-xylooligosaccharides from alkali pretreated mahogany and mango wood sawdust by using purified xylanase of *Clostridium* strain BOH3. Carbohydr Polym 167:158–166. <https://doi.org/https://doi.org/10.1016/j.carbpol.2017.03.021>

Sato N, Furuta T, Takeda T, et al (2019) Antioxidant activity of proteins extracted from red alga dulse harvested in Japan. J Food Biochem 43:e12709. <https://doi.org/https://doi.org/10.1111/jfbc.12709>

Sheu WH-H, Lee I-T, Chen W, Chan Y-C (2008) Effects of Xylooligosaccharides in Type 2 Diabetes Mellitus. J Nutr Sci Vitaminol (Tokyo) 54:396–401. <https://doi.org/10.3177/jnsv.54.396>

Singh RD, Banerjee J, Arora A (2015) Prebiotic potential of oligosaccharides: A focus on xylan derived oligosaccharides. Bioact Carbohydrates Diet Fibre 5:19–30.

<https://doi.org/https://doi.org/10.1016/j.bcdf.2014.11.003>

Vardakou M, Dumon C, Murray JW, et al (2008) Understanding the Structural Basis for Substrate and Inhibitor Recognition in Eukaryotic GH11 Xylanases. J Mol Biol 375:1293–1305.

<https://doi.org/https://doi.org/10.1016/j.jmb.2007.11.007>

Viana AG, Noseda MD, Gonçalves AG, et al (2011)  $\beta$ -d-(1→4),  $\beta$ -d-(1→3) ‘mixed linkage’ xylans from red seaweeds of the order Nemaliales and Palmariales. Carbohydr Res 346:1023–1028.

<https://doi.org/https://doi.org/10.1016/j.carres.2011.03.013>

Yagi H, Takehara R, Tamaki A, et al (2019) Functional Characterization of the GH10 and GH11 Xylanases from *Streptomyces olivaceoviridis* E-86 Provide Insights into the Advantage of GH11 Xylanase in

Yamamoto Y, Kishimura H, Kinoshita Y, et al (2019) Enzymatic production of xylooligosaccharides from red alga dulse (*Palmaria* sp.) wasted in Japan. Process Biochem.  
<https://doi.org/https://doi.org/10.1016/j.procbio.2019.03.030>

Zhu S, Wu Y, Yu Z, et al (2006) The effect of microwave irradiation on enzymatic hydrolysis of rice straw. Bioresour Technol 97:1964–1968. <https://doi.org/https://doi.org/10.1016/j.biortech.2005.08.008>

Zhu Z-Y, Zhao L, Ge X-R, et al (2015) Preparation, characterization and bioactivity of xylobiose and xylotriose from corncob xylan by xylanase. Eur Food Res Technol 241:27–35.  
<https://doi.org/10.1007/s00217-015-2431-0>

## Tables

Table 1 Kinetic parameter of StXyl10 and StXyl11					
Enzyme	Substrate	$K_m$	$V_{max}$	$k_{cat}$	$k_{cat}/K_m$
		mg/ml	μmol/min/mg	/sec	sec/(mg/ml)
StXyl10	GX	3.42	2,947	2,308	675
	DX	3.52	3,587	3,020	858
StXyl11	GX	14.2	16,286	8,685	610
	DX	12.0	10,233	5,338	445

Table 2 Hydrolysis of DX by StXyl10 and StXyl11

Enzyme	Hydrolysis conditions and Products	Relative value				
StXyl10	( $\mu$ g/ml) and 4 h	0.1	0.2	0.5*	1.0	2.0
	X1	0.989	0.957	1.000	1.165	1.222
	DX	1.212	1.087	1.000	0.898	0.829
	Time (h) and 0.5 $\mu$ g/ml	1	2	4*	12	
	X1	0.976	1.001	1.000	1.421	
	DX	1.363	1.273	1.000	0.995	
StXyl11	( $\mu$ g/ml) and 24 h	0.5	1.0	2.0*	4.0	8.0
	X1	0.990	0.994	1.000	1.050	1.100
	DX	1.020	1.012	1.000	0.977	0.982
	Time (h) and 2.0 $\mu$ g/ml	1	12	24*	36	
	X1	1.067	1.022	1.000	1.019	
	DX	1.272	1.109	1.000	0.980	

\*, The conditions are expressed as 1.000 for standards.

Relative values are obtained by the density of TLC.

Hydrolysis by StXyl10 and StXyl11 are performed in 10 mM sodium phosphate (pH 6.5) at 50 °C and 60 °C, respectively.

Table 3 Hydrolysis of DX by successive reaction with StXyl10 and StXyl11

Enzyme / Product	Hydrolysis conditions / Relative value				
StXyl10	0.5 µg/ml, 4 h				
StXyl11	None	0.5 µg/ml	2.0 µg/ml	24 h	36 h*
X1		1.056	1.011	0.983	1.002
DX		1.918	1.580	1.077	1.131

Relative values are obtained by the density of TLC.

\* , The conditions are expressed as 1.000 for standards.

Hydrolysis by StXyl10 and StXyl11 are performed in 10 mM sodium phosphate (pH 6.5) at 50 °C and 60 °C, respectively.

## Figures

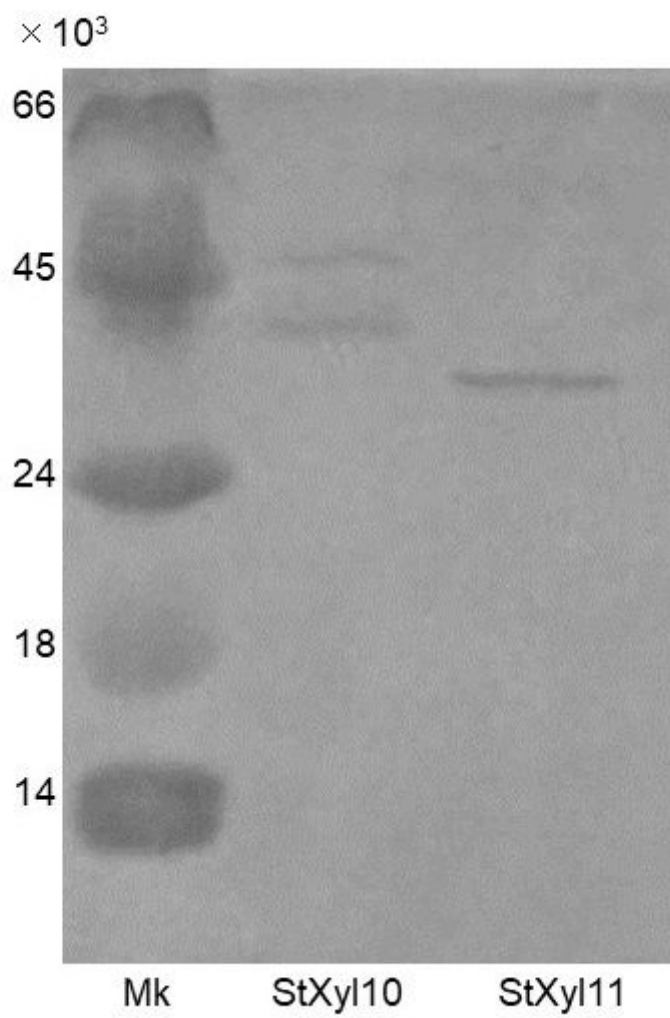


**Figure 1**

SDS-PAGE of purified xylanases. SDS-PAGE is performed by 15% acrylamide gel and applied 1  $\mu$ g of the purified enzymes.

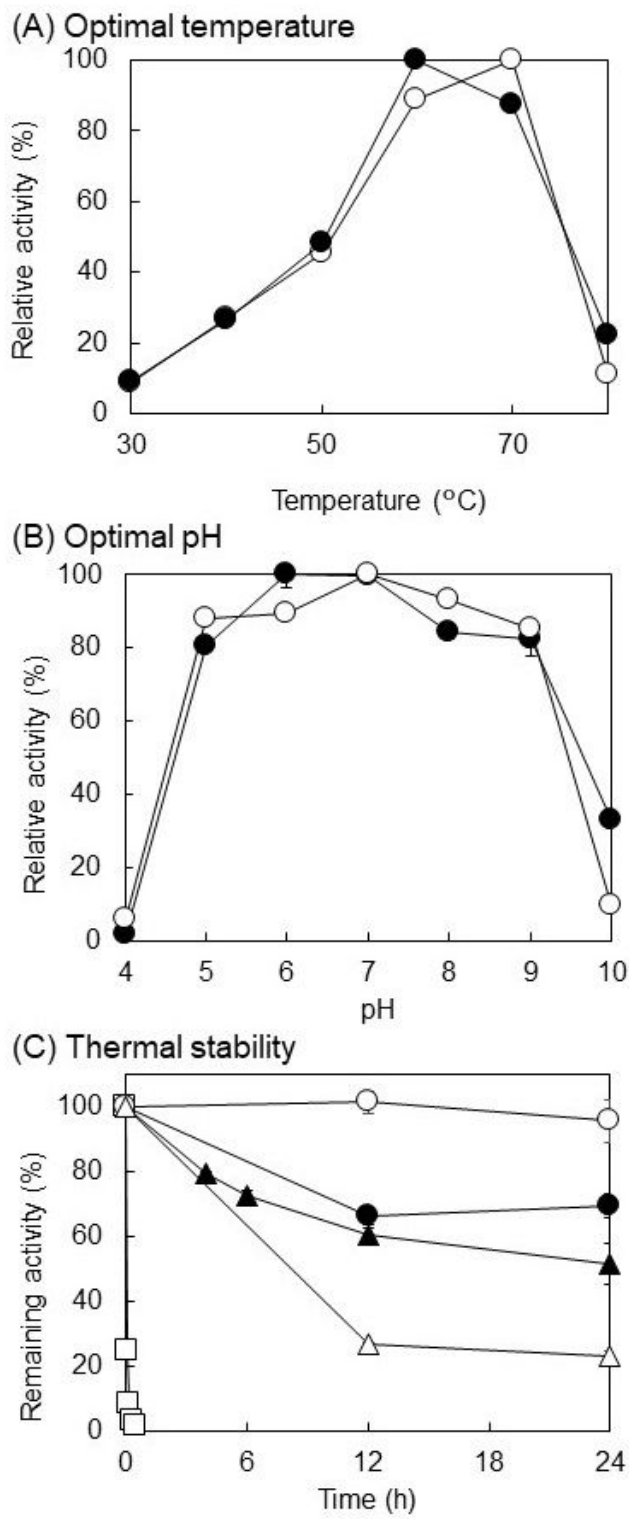


**Figure 2**

Optimum temperature and pH, and thermostability of StXyl10 and StXyl11. (A) Optimum temperatures of StXyl10 and StXyl11. The activities were measured at 30 – 80 °C in a reaction mixture containing 10 mg/ml of GX. □, StXyl10; ●, StXyl11. (B) Optimum pH of StXyl10 and StXyl11. The activities were measured at 65 °C in the reaction mixtures adjusted to pH 4.0 – 10.0. □, StXyl10; ●, StXyl11. (C) Thermal stabilities of StXyl10 and StXyl11. The remaining activities were assessed after the incubation of enzyme

at 50 – 70 °C for up to 24 h in 10 mM sodium phosphate buffer (pH 6.5). Average values for the triplicated measurements are shown with standard deviations.  $\square$ , StXyl10 at 50 °C;  $\triangle$ , StXyl10 at 60 °C;  $\square$ , StXyl10 at 70 °C;  $\bullet$ , StXyl11 at 50 °C;  $\blacktriangle$ , StXyl11 at 60 °C.

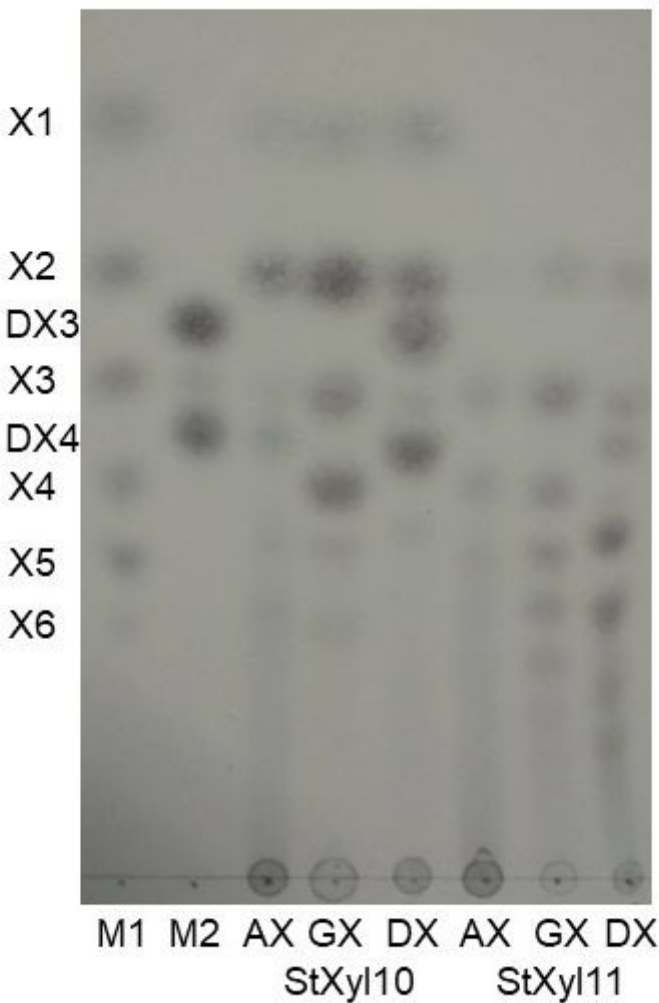


**Figure 3**

TLC for the hydrolysis products of xylan by StXyl10 and StXyl11. Ten mg/mL of xylan (AX, DX and GX) in 10 mM sodium phosphate buffer (pH 6.5) are hydrolyzed with 1.0  $\mu$ g/ml of StXyl10 at 50 °C for 24 h and 1.0  $\mu$ g/ml of StXyl11 at 60 °C for 24 h. One  $\mu$ L of the mixture was applied to TLC. M1, marker of X1-X6; M2, marker of DX3 ( $\beta(1\rightarrow3)$  xylosyl xylobiose) and DX4 (xylotetraose having one  $\beta(1\rightarrow3)$  xylosyl linkage); AX, arabinoxylan; DX, dulse xylan; GX glucuronoxylan.

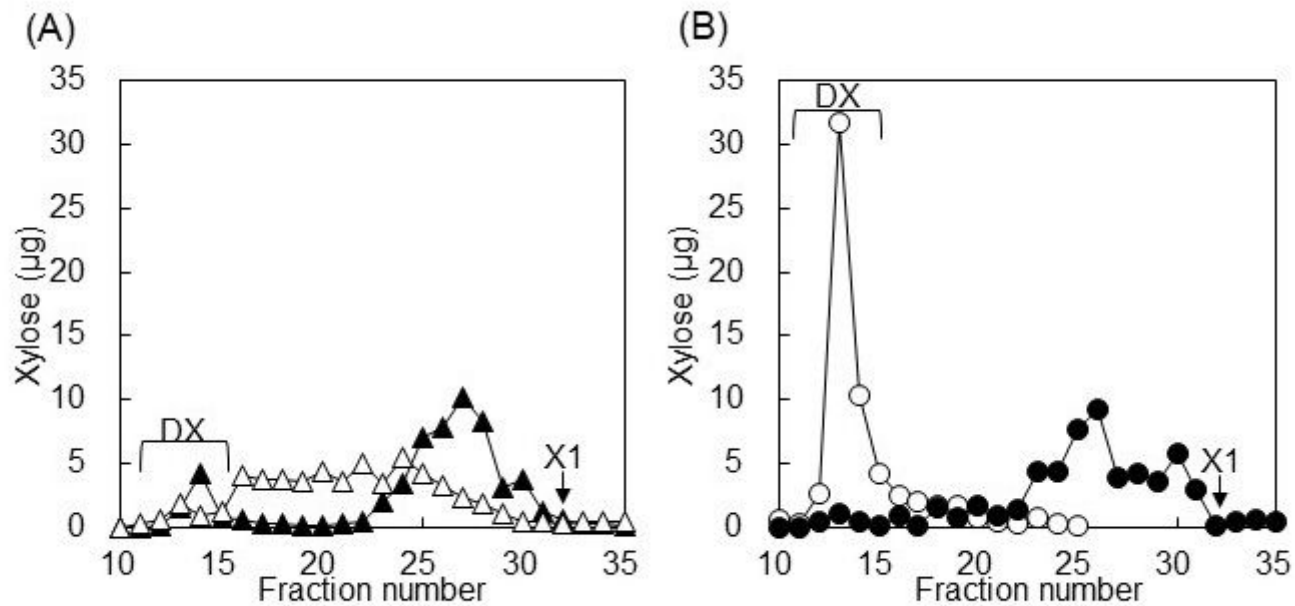


**Figure 4**

Gel filtration of DX and the hydrolysates from StXyl10, StXyl11 and their combination. The hydrolysates are separated by Superdex peptide 10/300 GL column. The amounts of each sugar are detected by phenol-sulfate method. (a), ●, DX; ●, StXyl10 and StXyl11; (b), △, StXyl10; □, StXyl11.

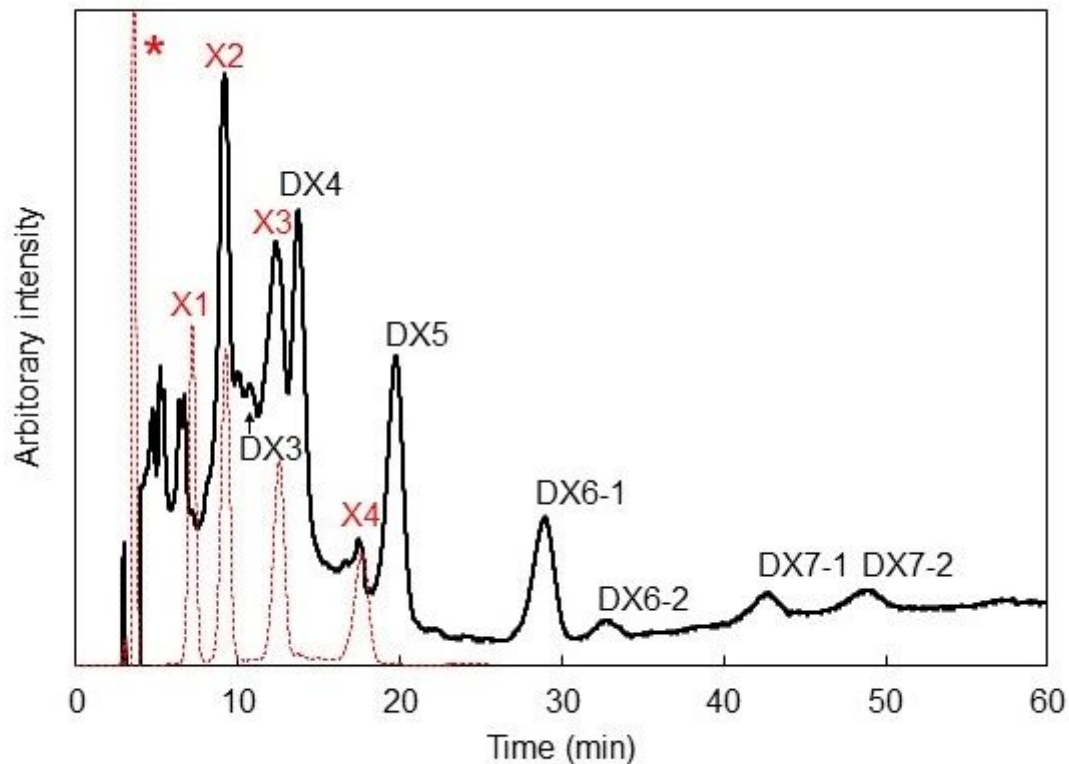


## Figure 5

Chromatogram of the hydrolysate from StXyl10 and StXyl11. The hydrolysate is separated by Sugar-D column (4.6×250 mm) with a flow rate of 1.0 ml/min using isocratic elution with 75% acetonitrile and detected by RI detector. Standards, X1 – X4 and DX3 and DX4. DP of sugar peaks eluted later than X4 (DX5 – DX7-2) are estimated by their retention times.

## Supplementary Files

This is a list of supplementary files associated with this preprint. Click to download.

- [Graphicabstract2.pptx](#)